JOURNAL of
MATERIALS and MECHATRONICS:A

e-ISSN 2717-8811
JournalMM, 2022, 3(2), 257-274
https://doi.org/10.55546/jmm.1188617

Araştırma Makalesi / Research Article

Numerical Investigations on Operation Modes and Transients of IPM Machines with Dual Windings

Tayfun GUNDOGDU[1, 2]*

[1] Hakkâri Üniversitesi, Mühendislik Fakültesi, Elektrik-Elektronik Mühendisliği Bölümü, Hakkâri, Türkiye
[2] GAMAK Makina Sanayi A.Ş., Dudullu OSB, Baraj Yolu Cad. No:2 34776 Ümraniye/İstanbul, Türkiye
ORCID ID: https://orcid.org/0000-0002-7150-1860, tgundogdu@gamak.com

Geliş/ Received: 13.10.2022; **Kabul / Accepted:** 07.11.2022

ABSTRACT: This paper investigates the flux-weakening characteristics and transient response of a dual winding interior permanent magnet (DWIPM) machine designed using the 2010 Toyota Prius IPM Machine specifications. In order to thoroughly adjust the main flux, dual windings are fed by separate identical inverters. Thus, significantly high-torque for high-speed requirements can be simply achieved by making one of the inverters open-circuited. Transient response of the DWIPM machine, including torque and current pulsations, occurring during normal drive or deactivation of one of the inverters has also been investigated for different operation modes. The flux-weakening performance characteristics of the proposed DWIPM machine have been compared with those of its single-fed counterpart in order to highlight the benefits and drawbacks of the dual-winding topology. The steady-state performance characteristics, torque/speed and power/speed curves, efficiency maps, machine transient response, different machine design options with various numbers of turns per phase and current amplitudes, and the importance of the electromagnetic coupling between dual windings have all been addressed. For transient and steady-state analyses, 2D, nonlinear, time-stepping finite element method (FEM) has been employed. It has been revealed that the proposed DWIPM machine exhibit significantly improved flux-weakening characteristics, particularly high-power at constant power region and high efficiency at constant torque region, and quite low current and torque pulsations occurring during operation mode change.

Keywords: Flux-Weakening, Interior Permanent Magnet Machine, Dual Winding Topology, Traction Application, Transient Response.

*Sorumlu yazar / Corresponding author: tgundogdu@gamak.com

Bu makaleye atıf yapmak için /To cite this article

Gundogdu T. (2022). Numerical Investigations on Operation Modes and Transients of IPM Machines with Dual Windings. Journal of Materials and Mechatronics: A (JournalMM), 3(2), 257-274.

1. INTRODUCTION

In recent years, the flux-weakening capability of an electric machine has grown increasingly crucial in specific applications such more electric vehicles, aircraft, rail traction, and ship propulsion. It is frequently necessary to increase an electric machine's speed control range. The highest possible inverter voltage, and consequently the voltage that is available for a particular back-electromotive force (EMF) amplitude, set a limit on the speed. In the case that the motor is fed by an inverter using voltage to frequency (V/f) regulation, the speed range is roughly two to three times the base speed (Dubey, 1989). The flux-weakening concept, machine parameter changes, and inverter rating can all be used to some extent to extend the speed range.

Many different methods have been proposed to improve the flux-weakening capability of electric machines. Among these methods, winding reconfiguration/changeover and number of turn change techniques (Swamy et al., 2005; Maemura et al., 2005; Kume et al., 1991; Gündoğdu, 2022) and double fed or dual inverter method (Tang et al., 2017; Takatsuka et al., 2014; Fuchs et al., 2008; Schraud et al., 2008; Hijikata et al., 2012; Lin et al., 2020) are the most popular ones. The electrical winding changeover technique is an effective way to extend the speed control range (Kume et al., 2004; Swamy et al., 2005; Maemura et al., 2005; Kume et al., 1991; Gündoğdu, 2022). Making the power losses in the converter as modest as feasible is another crucial factor to take into account for motor drive systems (Gündoğdu, 2022; Tang et al., 2017; Takatsuka et al., 2014). In (Gündoğdu, 2022), the windings number of turn change method has been successfully implemented into an IPM machine and a significantly improved torque at constant power region and increased efficiency at constant torque region has been achieved. It has been reported in (Tang et al., 2017) that the reconfigurable windings enable a reduction in motor size for a given power rating as well as an increase in motor output power for a given size, while also enhancing system drive cycle efficiency. In order to achieve high efficiency motor driving, (Takatsuka et al., 2014) describes an electronic winding changeover technique that effectively controls the low- and high-speed winding modes. Using electronic switches, it has been suggested in (Fuchs et al., 2008) and (Schraud et al., 2008) to increase the speed range by reconfiguring the windings in real-time. The windings can be switched from one containing a variable number of poles to another, or from one connecting in series to another, depending on how many turns are in each phase. In a similar study (Hijikata et al., 2012), an online winding reconfiguration method is proposed to change the winding layout from conventional to concentrated or vice versa in order to change the motor's whole characteristics. Moreover, the winding reconfiguration method is utilized for a line-start permanent magnet machine to improve the starting and steady-state performance characteristics (Lin et al., 2020).

A comprehensive study on double-fed IPM machines has been presented in (Gundogdu, 2022). It is reported that the proposed double winding with double inverter topology provides a good field-regulation capability without magnet demagnetization. In (Fukuda et al., 2019) and (Barcaro et al., 2010), a multi-phase double-winding permanent magnet machine with an integrated inverter is proposed to reduce the current per output power, extend speed range and also to increase the fault tolerance. Moreover, improved drive characteristics, fault-tolerant features, and redundancy of a double-winding permanent magnet machine have been experimentally shown (Noguchi et al., 2018).

By switching the coil arrangement from series to parallel or altering the number of turns per coil, windings can be reconfigured in order to alter the flux-weakening properties. This could result in losses directly correlated to rotor speed due to an undesired voltage unbalance between winding

groups and circulating currents, or even failures. Therefore, transient response and circulating currents for machines with reconfigurable or dual windings have been studied by many researchers (Copt et al., 2015; Daniels et al., 2019; Im et al., 2019; Sin et al., 2020; Sadeghi et al., 2012).

In this study, the flux-weakening capability and also the efficiency map of an IPM machine having dual windings have been investigated together with transient response during operation mode change. Activation of windings according to different operation modes has been determined for different maximum current levels. In addition, how to design a cost-effective drive with inverters having low current levels is presented. The main idea behind dual winding and inverter topology is to change the number of turns of windings and hence change the inductance in order to reduce the level of induced voltage and consequently increase the torque level at constant power region by keeping the current level at high. Firstly, the steady-state and the flux-weakening performance characteristics, including torque/speed curves, power/speed curves and efficiency maps of the DWIPM machine have been calculated and compared to its single-fed counterpart. Then, transient responses, including phase current and torque pulsations, occurring during operation mode change have been investigated. It has been found that significantly improved flux-weakening characteristics can be achieved thanks to the proposed topology. In addition, the significant level of torque and current pulsations occurring during operation mode change can be minimized by gradually changing the current level of inverters.

2. OPERATION MODES AND STEADY-STATE PERFORMANCE

2.1 Design Specifications and Steady-State Performance

Dual windings, each accommodated in the same stator slots and fed by separate inverters, are proposed in order to alter the main flux and so enhance the flux-weakening capability of an IPM machine. The proposed IPM machine is designed using the primary geometric and operational requirements of the Toyota Prius 2010 IPM machine which has 48-stator slot, 8-pole and conventional (integer slot distributed winding) single-layer windings. Note that the dual winding counterpart (proposed) IPM machine of the Toyota Prius 2010 IPM machine has the identical winding layout. The design specifications, material properties and also the some key steady-state performance characteristics of the proposed IPM machine is listed in Table 1. The 2D view of the proposed IPM machine's model, mesh structure and also the steady-state flux distributions are shown in Figure 1(a), (b), (c) and (d), respectively. In addition, the BH curve and core loss characteristics for various frequencies are illustrated in Figure 2. For the numeric calculations, the ANSYS Electronics program, which is based on the 2D, non-linear, time-stepping finite element method (FEM), is employed to calculate the transients and steady-state characteristics. Note that once both windings (main and aux) are excited simultaneously, the proposed IPM machine works as a conventional single three phase machine. More details about the operation modes of the proposed IPM machine is given in Section 2.2.

Table 1. Design, operating, and material specifications of the IPM machine together with the steady-state (rated) performance characteristics

Parameter	Unit	Value
Phase Current	A	236
Max. Inverter Voltage	V	650
Rated Speed	rpm	950
Rated Torque	Nm	222
Torque Ripple @ 950 rpm	%	8.43
Back-EMF Amplitude @ 950 rpm	V	65

Table 1. (Continued) Design, operating, and material specifications of the IPM machine together with the steady-state (rated) performance characteristics

Parameter		Unit	Value
Back-EMF THD @ 950 rpm		%	14.3
Efficiency @ 950 rpm		%	~81
Max. Speed		rpm	20000
Stator Outer Diameter		mm	264
Stator Inner Diameter		mm	161.9
Stator axial length		mm	50.8
Rotor Inner Diameter		mm	51
Air-gap		mm	0.73
Number of Slot			48
Turns per coil			11
Parallel brunches			2
Coils in series per phase			8
Number of turns per phase			88×2
PM dimensions (W× T)		mm^2	35.76×7.16
Slot fill factor			0.45
Core Material			M270-35A
	Hysteresis loss coefficient (K_h)		179.04
	Classical loss coefficient (K_c)		0.375
	Excess loss coefficient (K_e)		0.262
	Mass density (ρ)	kg/m^3	7650
	Stacking factor (K_{fe})		0.93
PM material			NdFeB35
	Permeability		1.05
	Conductivity (σ)	s/m	625000
	Coercivity (H_c)	A/m	-805399.8
	Mass density ρ	kg/m^3	7607

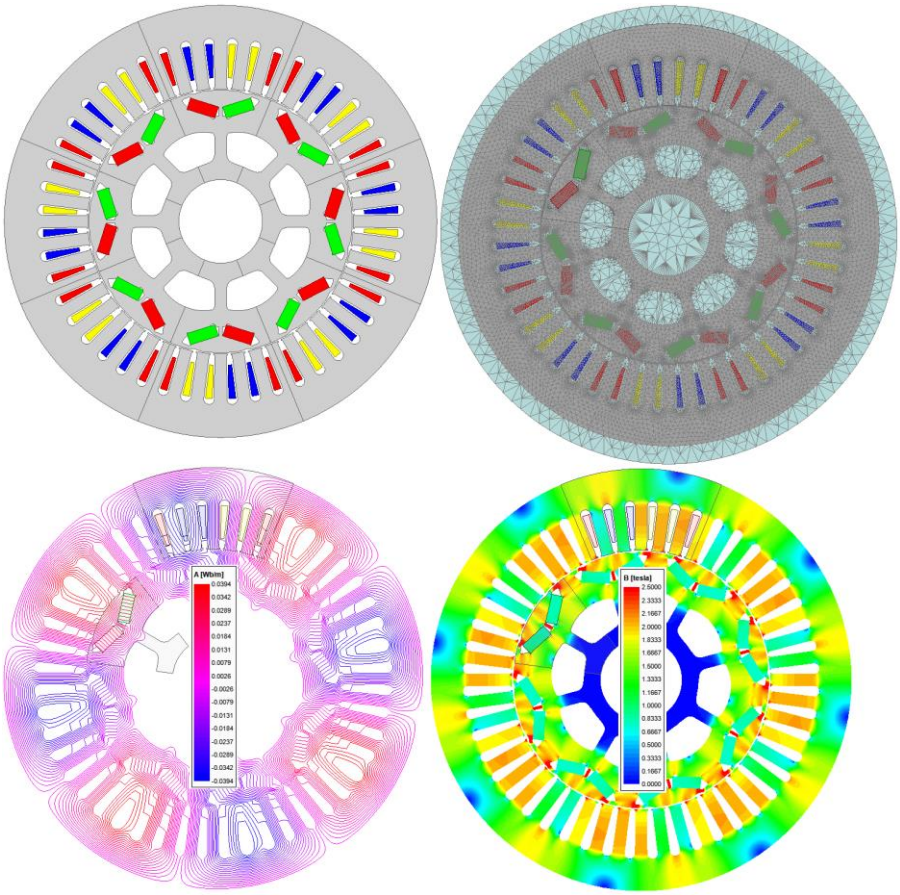

Figure 1. Machine model and magnetic field distributions: (a) IPM Machine model; (b) mesh stracture; (c) magnetic flux distribution; (d) flux density distributions

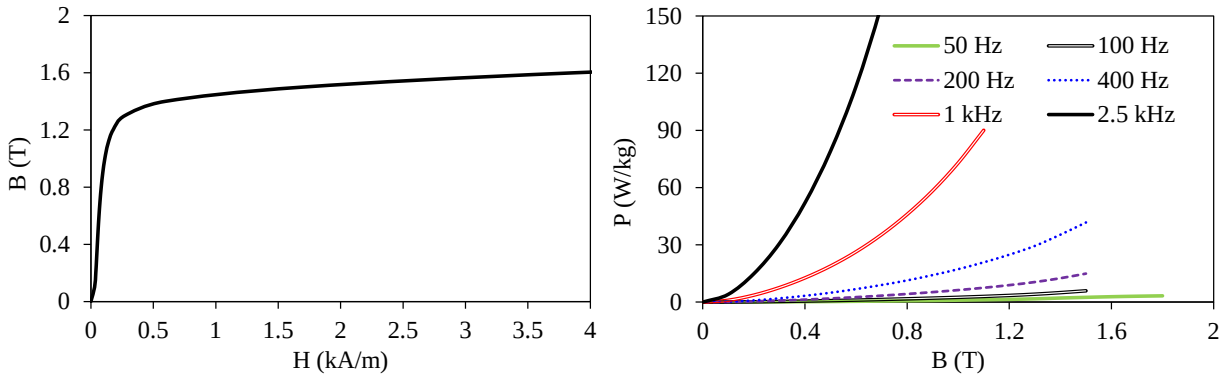

a) BH curve b) Loss curve

Figure 2. Magnetic properties of M270-35A core material

2.2 Operation Modes

In order to drive the DWIPM machine in accordance with traction applications, the IGBT inverters, consisting of IGBT power modules to assure high frequency and voltage/power switching operations, can be utilized. Depending on the inverters' maximum current, it is feasible to determine the number of turns for the windings. The same torque amplitude can be obtained by utilizing a parallel branched winding arrangement because the output torque is a function of MMF, or indeed the number of turns multiplied by current amplitude. Thus, cheaper excitation system (batteries and inverters) with low current levels can be utilized to operate the machine without sacrificing the torque amplitude. The both topologies have been shown in Figure 3. As can be seen, it is possible to operate the proposed dual winding IPM machine by connecting the identical inverters in parallel and changing the excitation current level. Thus, high efficiency at low-speed (cruise mode) operation and high-power at high-speed operation mode can be achieved.

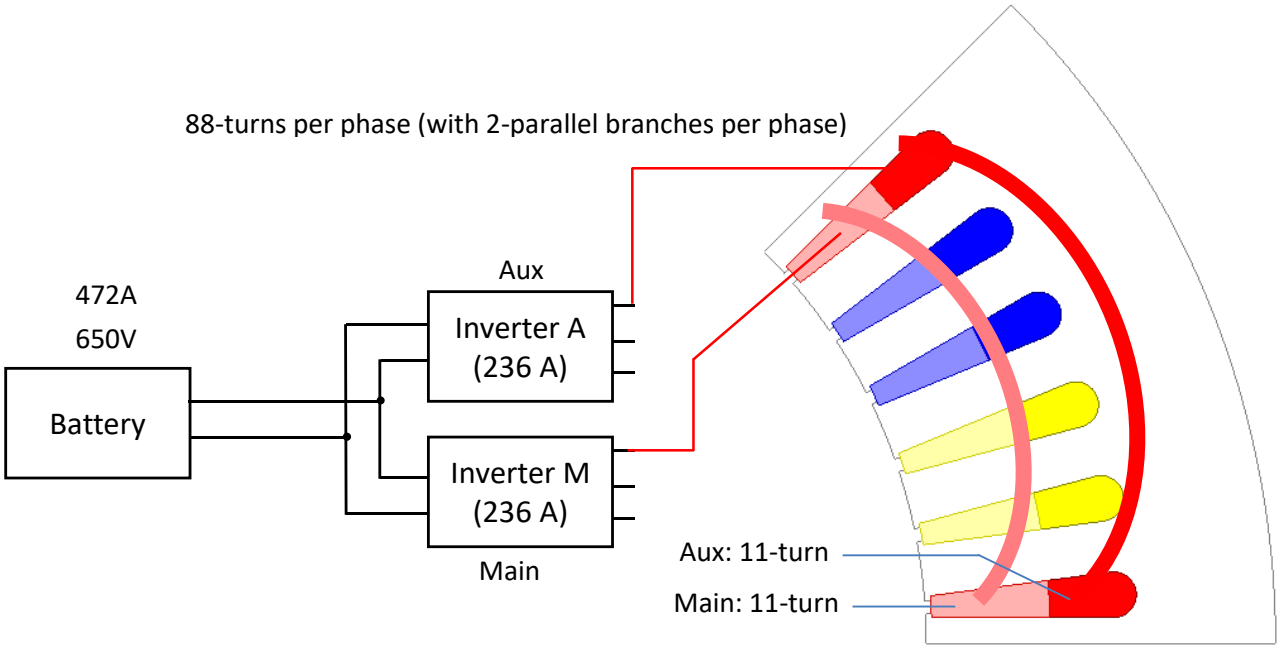

a) 236A Inverter (DWIPM-1)

Figure 3. Parallel connected identical inverters for improved flux-weakening capability and redundancy

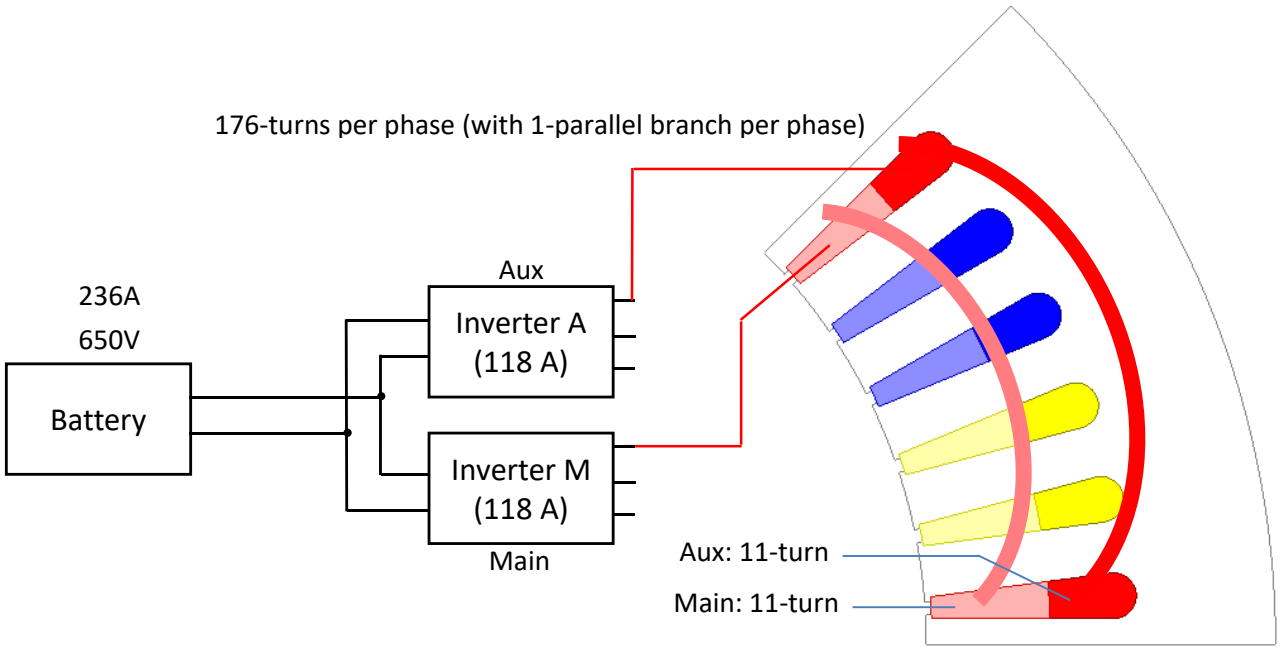

b) 118A Inverter (DWIPM-2)

Figure 3. (Continued) Parallel connected identical inverters for improved flux-weakening capability and redundancy

Different operation modes and corresponding inverter current (I_{max}) rates and also the phase resistance (R_{phase}) and the maxsimum torque (T_{max}) amplitudes are given in Table 2. Note that 'M//A' indicates that the main 'M' and auxiliary 'A' windings are connected parallel through the inverters and excited simultaneously. As can be seen, thanks to the dual windings, it is possible to obtain cruise, hill climbing, and high-speed modes. Depending on the road conditions, the possible highest efficiency can be achieved thanks to the orientation of the active winding and hence the inverter. Each winding group has 11-turn per phase with 2-parallel branches. Therefore, the total number of serial turns per phase is 11. As seen in Figure 3, two identical inverter whose maximum current rates are 236A is used for each winding group. Note that, if the battery current is limited to 236A (see Figure 3(a)), then the maximum inverter current rate can be reduced to half. However, in order to maintain the torque, the number of turns should be doubled. It can be done easily by reducing the parallel branch number from two to one. Thus, all the electromagnetic performance characteristics will remain the same for the constant torque region. However, since the voltage requirement is doubled, theoretically, the power at high speed will be halved. If the inverter voltage doubled (2×650V), then the similar performance with the 236A excitation can be obtained. Moreover, it is advantageous to use more stranded windings in terms of avoiding extra eddy current losses at high-speed operations.

Table 2. Operation modes and corresponding inverter currents at constant torque region

		Mode	Active Winding	I_{max} per inverter (A)	R_{phase} @ 100°C (Ω)	T_{max} @ 1krpm (Nm)
472A DWIPM-1	1	Cruise 1	M//A	59	0.0248177	64.61
	2	Cruise 2	M//A	118	0.0248177	136.33
	3	Hill	M//A	236	0.0248177	239.3
	4	High-Speed 1	M	236	0.04737	139.3
	5	High-Speed 2	M	118	0.04737	65.03
236A (k_{fill} = 0.448) DWIPM-2 (650V)	1	Cruise 1	M//A	29.5	0.10087	64.61
	2	Cruise 2	M//A	59	0.10087	136.33
	3	Hill	M//A	118	0.10087	239.3
	4	High-Speed 1	M	118	0.19248	139.3
	5	High-Speed 2	M	59	0.19248	65.03

As a conclusion, if very high-power is not required for the high-speed operations, then in order to reduce inverter cost and size; 118A design can be more reasonable candidate. The investigation of design with 118A (with doubled number of turns as shown in Figure 3(b) corresponding to DWPIM-1 in Table 2) has been considered in this study.

3. FLUX-WEAKENING CHARACTERISTICS ACCORDING TO OPERATION MODES

The torque/speed and power/speed characteristics, calculated based on Table 2 for various operation modes, are illustrated in Figure 4 and Figure 5, respectively. 'MA' indicates that both the main and auxiliary windings are excited simultaneously and 'M' indicates that only the main winding is excited. Note that the flux-weakening characteristics of 'MA (236A)' mode is identical to Toyota Prius 2010 IPM machine's performance. Because, as mentioned previous, once both windings are excited simultaneously with the maximum inverter current, it acts as a conventional single-fed machine. As seen in the figure, by reducing the current of the auxiliary winding to zero, it is possible to change to the number of turns from 88 to 44 per phase. Consequently, it is possible to achieve quite high power at high-speed operations. In the same manner, it is possible to achieve high torque at the constant torque region by simultaneously exciting the both the main and auxiliary windings with the maximum current (236A). Corresponding efficiency maps for each operation mode are illustrated between Figure 6 and Figure 8.

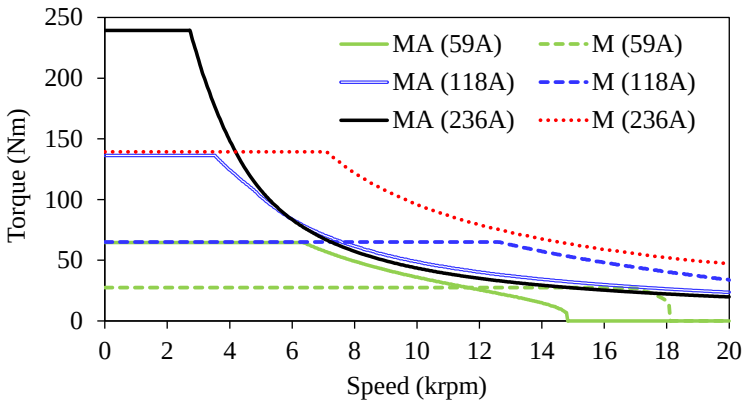

Figure 4. Torque/speed characteristics for different operation modes

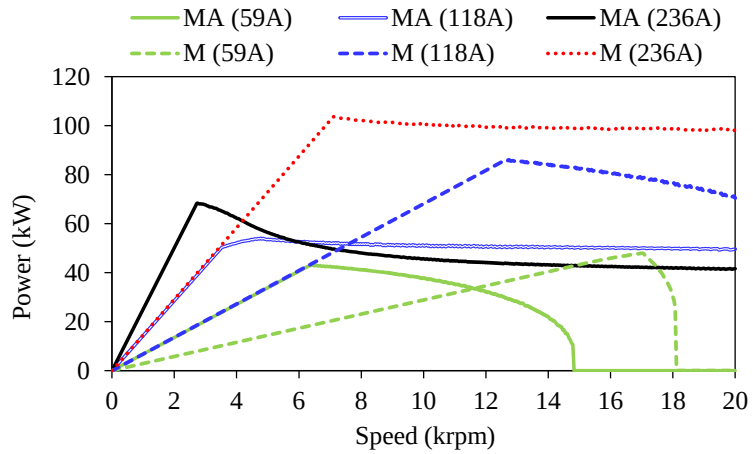

Figure 5. Power/speed characteristics for different operation modes

In order to determine which winding group excitation at low-speed operation mode has the advantage in terms of torque and efficiency, the torque/power-speed and efficiency maps can be compared. Considering efficiency map graphs, it can be deduced that at low-speed operations the 'MA' ensures higher torque and higher efficiency at the same current excitation level as the 'M'. In the same manner, at high-speed operations, excitation of the 'M' ensures higher torque and efficiency than that of the 'MA'.

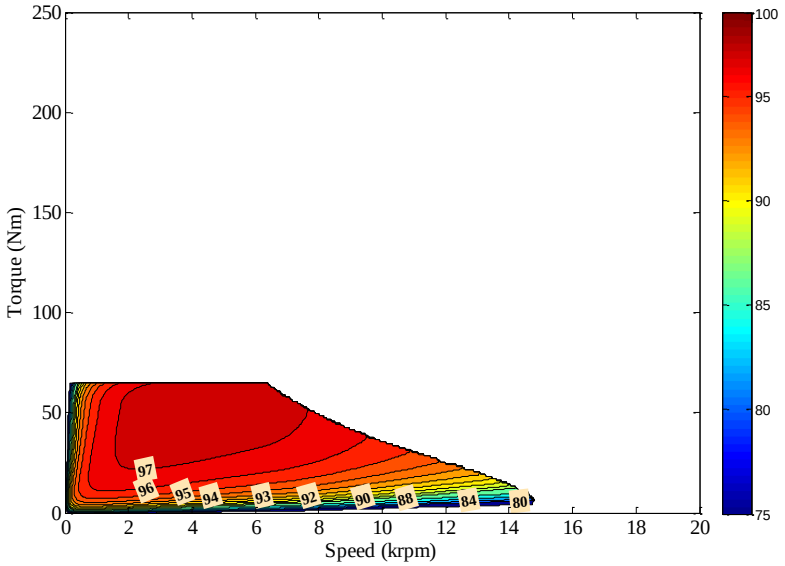

a) 'MA' (59A)

Figure 6. Efficiency map of 59A operation modes with (a) MA

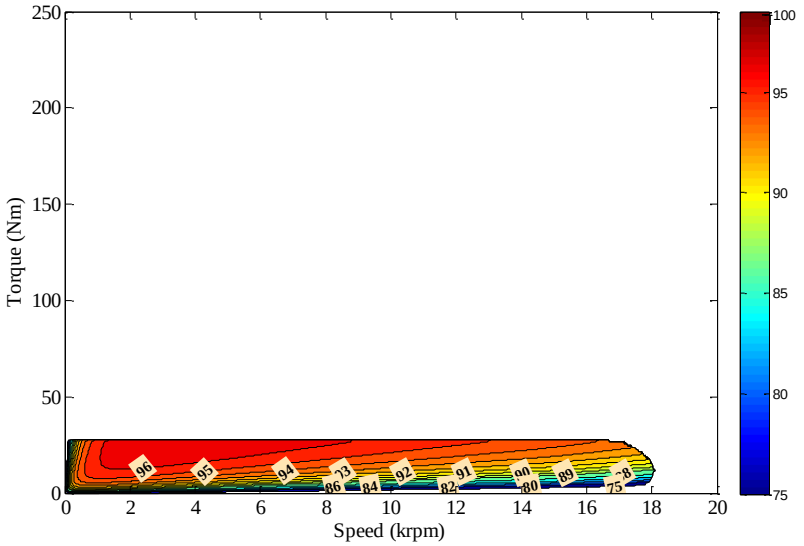

b) 'M' (118A)

Figure 6. (Continued) Efficiency map of 59A operation modes with (b) M

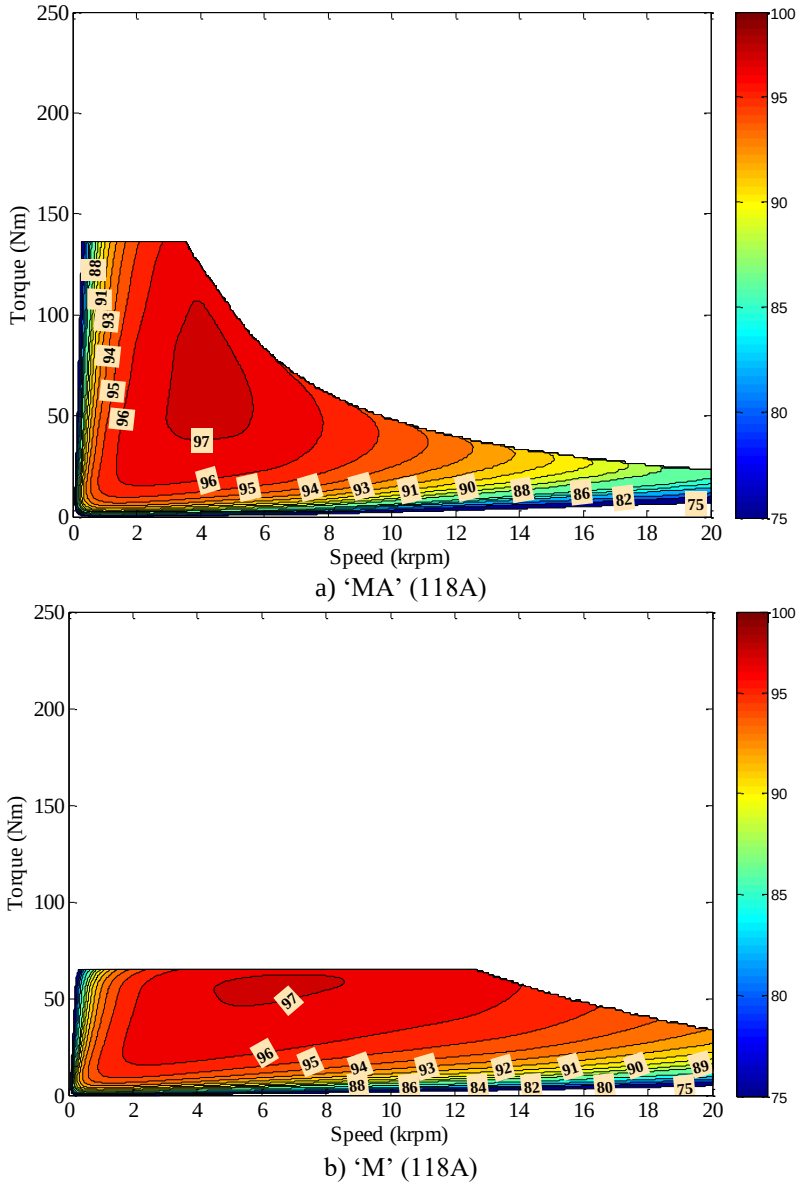

a) 'MA' (118A)

b) 'M' (118A)

Figure 7. Efficiency map of 118A operation modes with 'MA' (a) and 'M' (b)

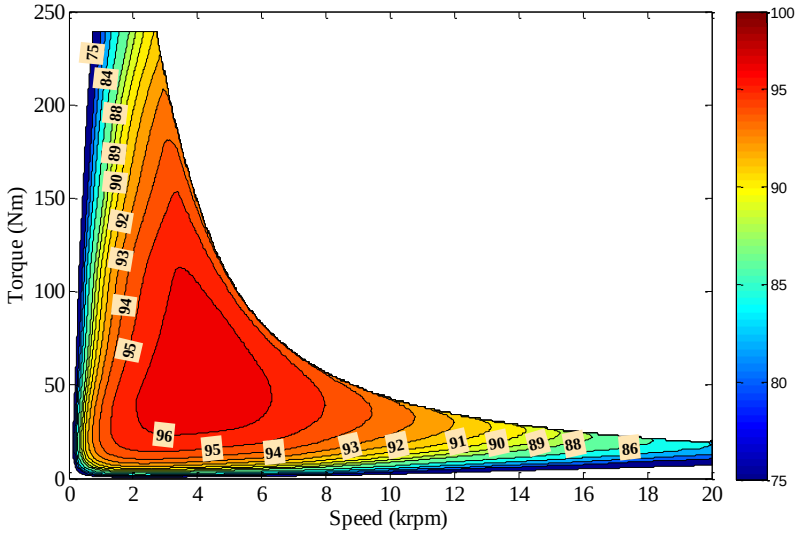

a) 'MA' (236A) and also original Toyota Prius IPM machine (ORG)

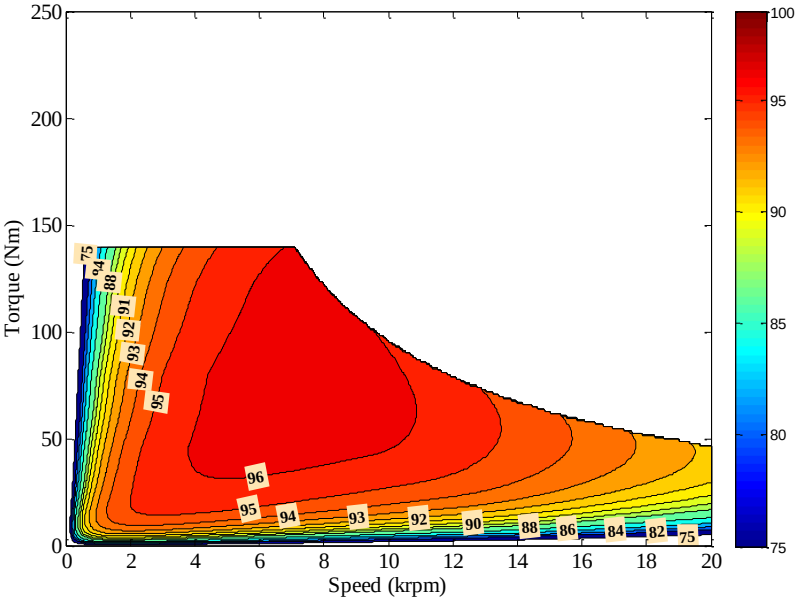

b) 'M' (236A)

Figure 8. Efficiency map of 236A operation modes with 'MA' (a) and 'M' (b)

In order to reveal the merits of the proposed method, the torque/power-speed characteristics of the DWIPM machine is compared with the original (ORG) IPM machine having conventional single 3-phase, single-layer windings and single inverter. It is obvious that thanks to the dual inverter drive, the maximum power at deep-flux weakening region is increased from ~40kW to ~100kW without sacrificing the maximum torque at the constant torque region as seen in Figure 9.

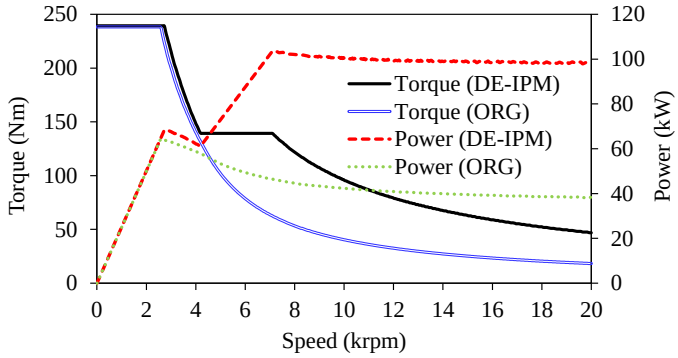

Figure 9. Integrated torque/power-speed characteristics

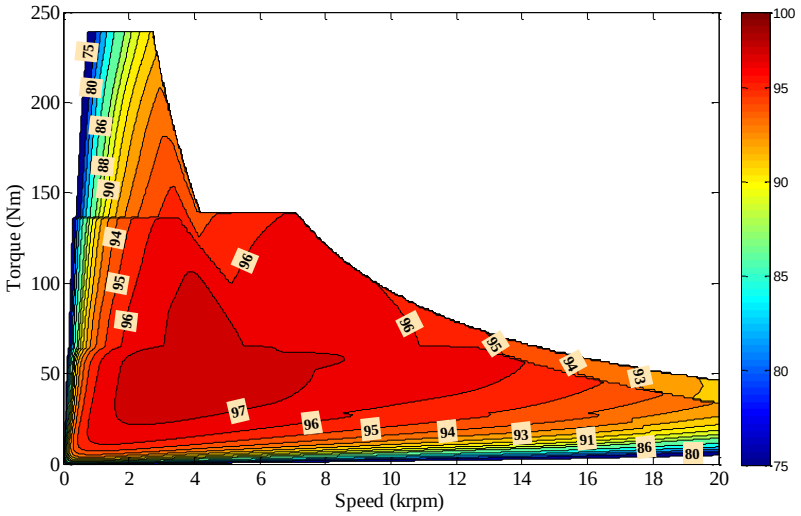

Figure 10. Integrated efficiency map showing all the available operation modes

The efficiency map, integrated from all the available operation modes, is shown in Figure 10. As clearly seen, 96% covers the larges area and the maximum efficiency is 97% achieved between ~1.8krpm and ~9krpm. Considering the original IPM machine's efficiency map (see Figure 8(a)), the efficiency at the cruise mode operation is increased significantly.

In conclusion, thanks to the proposed DWIPM topology, much higher efficiency in cruise mode and much higher power at the high-speed operation mode have been achieved when compared to single-excitation operation.

4. TRANSIENTS OCCURING DURING OPERATION MODE CHANGE

In this section, transient-state of the DWIPM machine during the operation mode change has been examined. Normally, the voltage and hence current level can be adjusted smoothly for operating mode changes by changing the voltage amplitude slowly. However, in some road conditions, fast voltage chance or winding changeover can be required. Therefore, it is necessary to investigate the transient response during operation mode changes. The electromagnetic torque and phase current transient responses during changing winding or voltage have been investigated by FEM. In order to observe the transients during the mode changes, different voltage injections have been assigned to the phase windings. Operating modes and corresponding phase current excitations are illustrated in Figure 11. Operating modes of the DWIPM is summarized as follows.

$\boxed{A}$ → Both inverters are active and the control is identical $I_A = I_M$
$\boxed{B}$ → Both inverters are active, the control is not identical $I_A = I_{max}$ and $I_M \to 0$
$\boxed{C}$ → Only one inverter feeding the main windings is active, $I_A = I_{max}$
$\boxed{D}$ → Only one inverter feeding the main windings is active, $I_A \to 0$

Note that I_A and I_M indicate the auxiliary and main winding inverter current amplitudes, respectively. Considering the operation modes and Figure 11, it can be deduced that transients occur only 'A' and 'B' regions since both inverters are activated.

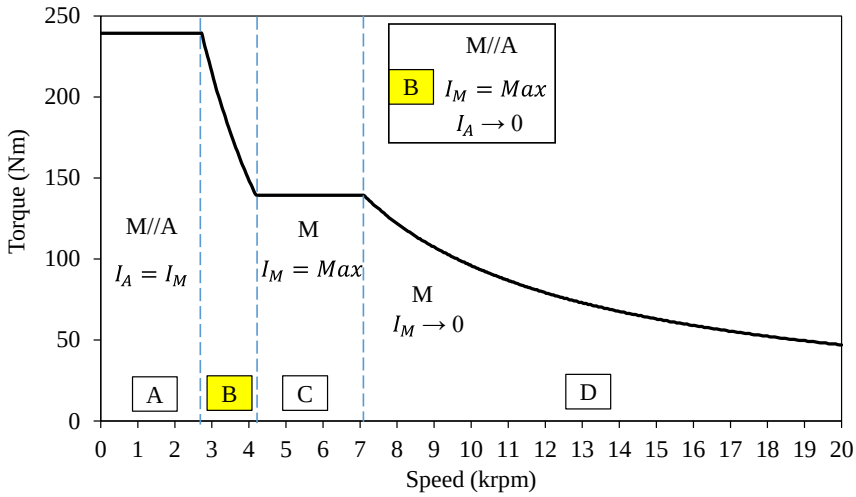

Figure 11. Operating modes and corresponding winding currents

4.1 Operation Region A

In this section, the transient response during region 'A' operation, illustrated in Figure 11, is investigated. The imposed speed is 1krpm and the maximum inverter current is taken as 118A. In order to observe the transient responses, the simulations have been set up to be run at (a) 29.5A and then (a') 63A peak current. The torque and phase current pulsations occurring during voltage change from (a) to (a') are illustrated in Figure 12 and Figure 13, respectively and summarized in Table 3. It can be observed that if the current is increased to its two times higher amplitude directly, very high pulsations occur. Therefore, it would be very safe to perform the operation mode changes should be done gradually with several steps. For instance, in order to avoid the high pulsations, ripples, faults, and any other devastating effects, instead of increasing the current from 29.5A to 59A directly, it can be increased by 5A by 6-steps. As seen in Figure 13, a very smooth transition can be obtained by gradually increasing the current amplitude. It has been shown that it is possible to reduce the torque pulsations ~5 times by increasing the current gradually rather than increasing the current according to direct current increment. Investigation of the pulsation for the 118A maximum inverter current is also investigated and the obtained results have been shown in Figure 14 and Figure 15. It has been revealed that once the current amplitude is increased, the fault time is shortened. The peak-to-peak (T_{p2p}) and average torque (T_{avg}) amounts are shown in Figure 14. Considering the findings presented for the operation region 'A', it can be deduced that in order to reduce the transient response and its effects, current regulation should be done by relatively small steps.

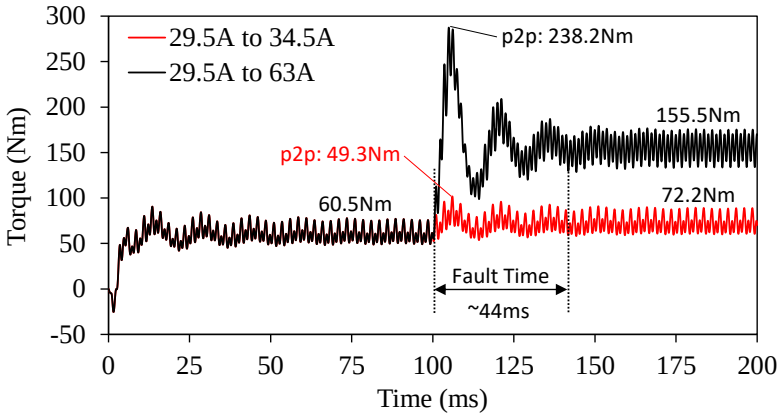

Figure 12. DWIPM machine electromagnetic torque and its transient response during the mode changing operation in region 'A'

Table 3. Torque and current pulsation percentages

State	I_{phase} Resultant	T_{ripple} (%) Before Fault	T_{p2p} (%) During Fault	T_{ripple} (%) After Fault	I_{p2p} (%) During Fault
(a)	29.5A → 34.5A	52.6	81.5/65.28	44.16	46.77/40
(a')	29.5A → 63A	52.6	393.72/153.2	30.6	423.7/198.4

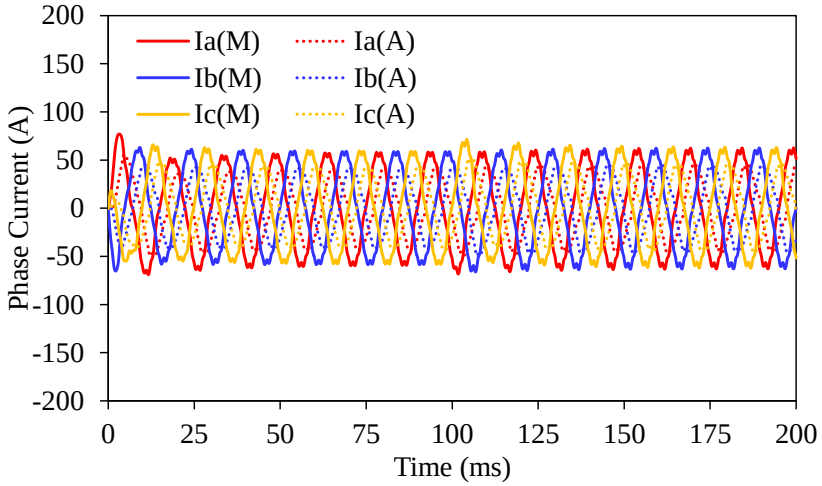

a) Phase current pulsation for the 29.5A→34.5A

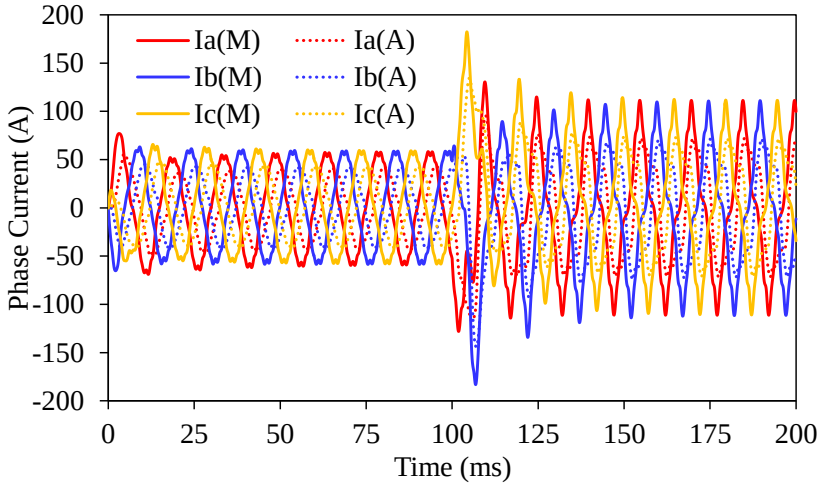

b) Phase current pulsation for the 29.5A→63A

Figure 13. Current pulsations during the mode change operation in region 'A'

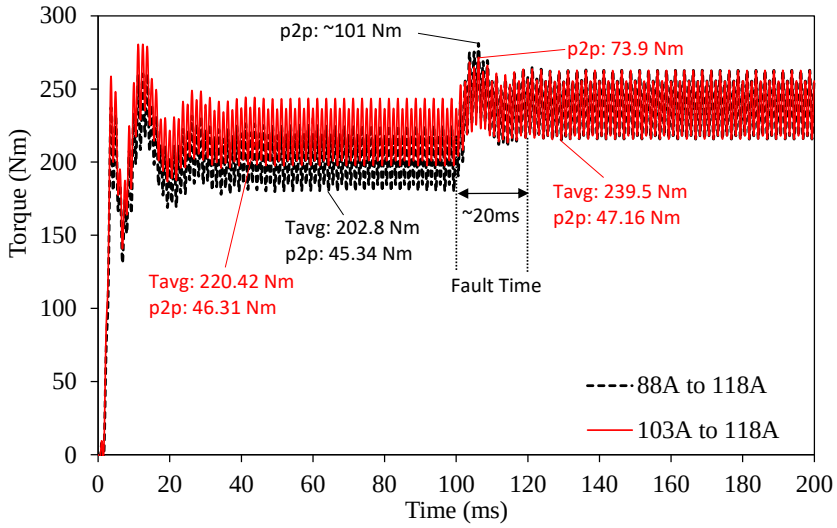

Figure 14. Torque pulsations for maximum inverter current

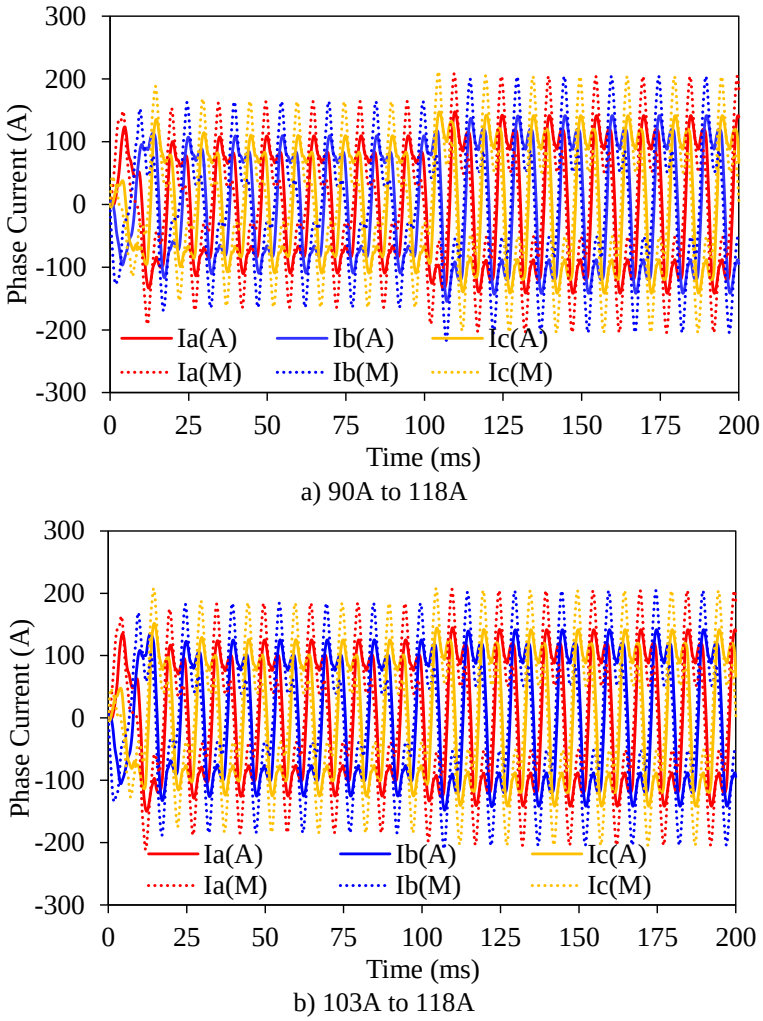

Figure 15. Current pulsations for maximum inverter current

4.2 Operation Region B

For the operation region 'B', the imposed speed is selected as 3krpm, and the maximum inverter current is taken as 118A. Since the inverters do not feed the windings with identical current amplitudes and angles, this operation region is the most critical operating region. Because of the coupling effect of the main and auxiliary windings (see Figure 16), a certain amount of voltage is induced in the auxiliary windings.

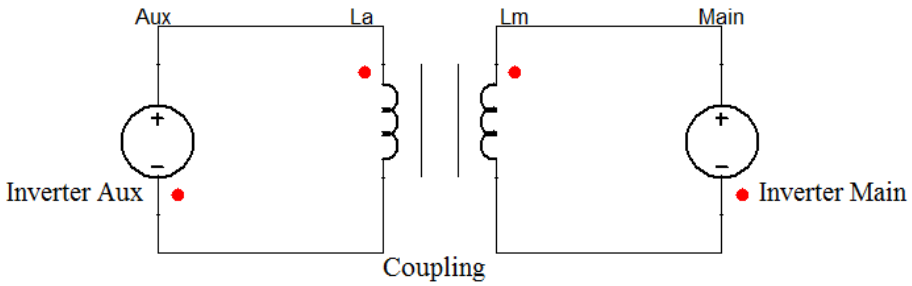

Figure 16. Schematic representation of coupling between the main and aux windings

In addition, if the amount of the induced voltage is higher than that of the inverter's voltage, the direction of the power is changed. Which means that if the current of the inverter is lower than that of the aux winding due to the coupling effect, inner circuit and circulating currents cause the inverter to failure. Therefore, an additional control algorithm is required in order to protect the

inverter from the induced voltage due to the coupling between the auxiliary and main windings. The torque and current pulsations that occurred during the operating mode change are shown in Figure 17 and Figure 18.

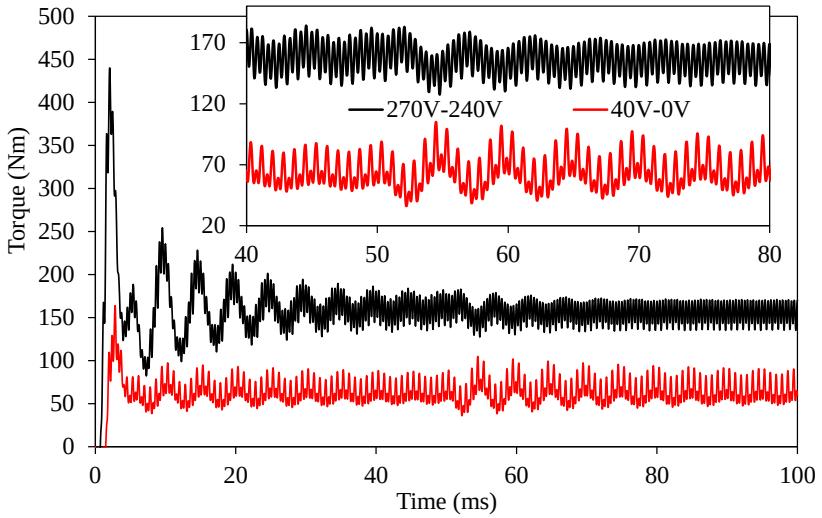

Figure 17. DWIPM machine electromagnetic torque and its transient response during the different mode changing operation

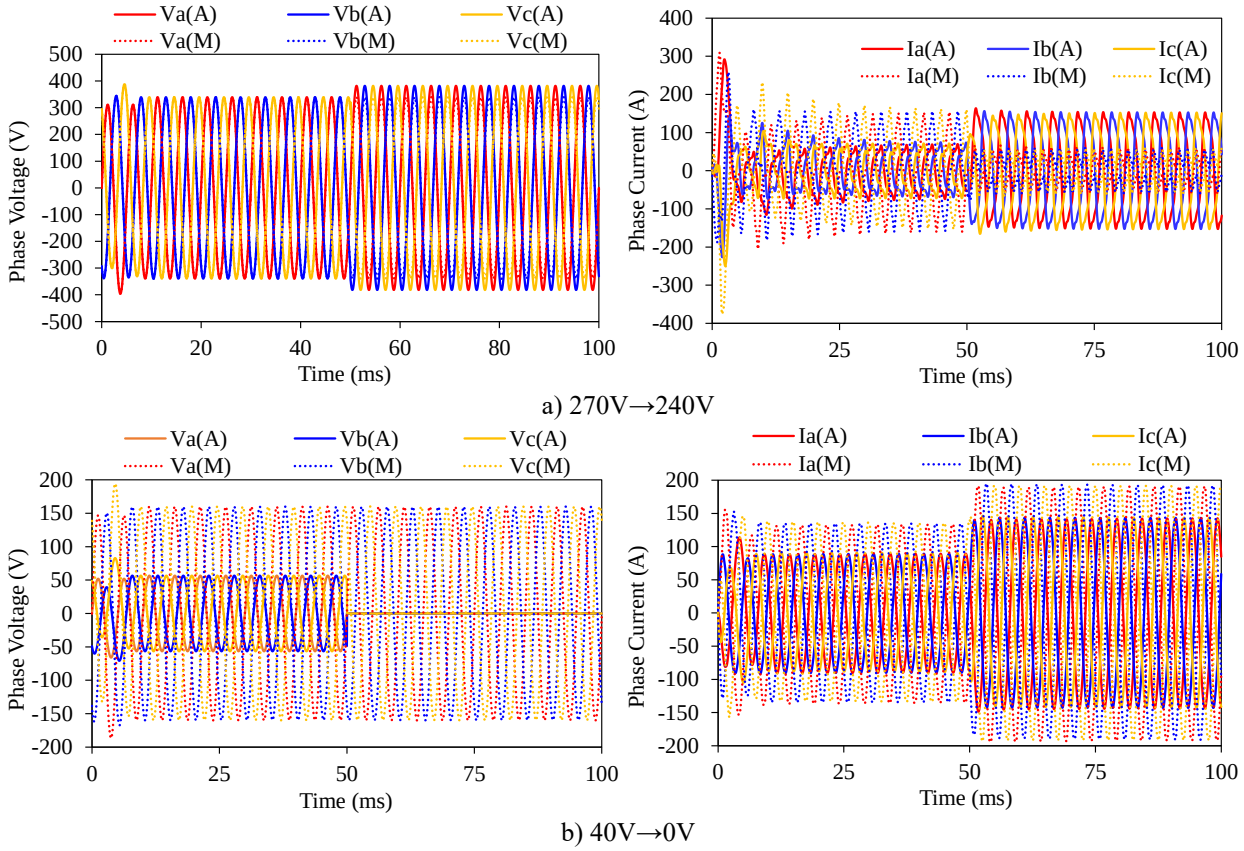

Figure 18. Current pulsations for maximum inverter current

As can be observed, in the operating region ‘B’, the amount of the current should be reduced in order to waken the flux. Therefore, while the main windings are fed with the maximum inverter voltage, the voltage of the auxiliary windings is reduced from 270V to 240V and 40V to 0V. As seen in the figures, the pulsations are not very high. On the other hand, as explained before, even if the

voltage of the auxiliary is reduced to 0V from 40V (inverter of the auxiliary winding should be open circuit for 0V), because of the coupling effect of the main windings, the current level of the auxiliary winding is increased. Therefore, it can be concluded that the inverter voltage of the auxiliary winding is already lower than the induced voltage of the auxiliary windings. Therefore, since the direction of the power is turned from the motor to the generator, the current coming from the inverter is decreased the amplitude. However, once the auxiliary inverter is open-circuited, the induced voltage of the auxiliary windings is increased (Figure 18(b)). Therefore, in order to avoid possible failures, an additional control algorithm should be added to the control scheme of the inverters for the operating region 'B'.

5. DISCUSSION ON FINDINGS AND CONCLUSION

In this study, a comprehensive investigation of the steady-state performance, flux-weakening characteristics, and transient response of an IPM machine with dual three–phase windings supplied by two parallel inverters have been presented. This dual winding strategy gives IPM machines an extra degree of control by allowing them to adjust the amount of series turns each phase and provides redundancy. It has been revealed that the reconfiguration of the IPM machine's windings with dual windings and excitation with dual inverters significantly improves the flux-weakening capability and makes it possible to minimize the transient torque and current during operation mode change. Thanks to the proposed dual winding topology, the followings have been achieved;

- Significantly improved torque/speed and power/speed characteristics;
- Significantly increased efficiency, particularly in cruise mode;
- Reduced transient response and its effects thanks to the current regulation by relatively small steps;
- Very smooth operating mode changes: it is possible to reduce the torque pulsations ~5 times via gradually incensement of current;

Moreover, it has been revealed that the circulating currents due to the coupling effect between the dual windings should be considered with care to avoid failures.

A synopsis of the future work includes demagnetization analyses and an investigation into the influence of the number of phases on the performance characteristics and transient response.

6. CONFLICT OF INTEREST

Author approves that to the best of his knowledge, there is not any conflict of interest or common interest with an institution/organization or a person that may affect the review process of the paper.

7. AUTHOR CONTRIBUTION

Tayfun GUNDOGDU has the full responsibility of the paper about determining the concept of the research, data collection, data analysis and interpretation of the results, preparation of the manuscript and critical analysis of the intellectual content with the final approval.

8. REFERENCES

Barcaro M., Bianchi N., Magnussen F., Analysis and Tests of a Dual Three-Phase 12-Slot 10-Pole Permanent-Magnet Motor. IEEE Transactions on Industry Applications 46(6), 2355-2362, 2010.

Copt F., Koechli C., Perriard Y., Minimizing the Circulating Currents of a Slotless BLDC Motor Through Winding Reconfiguration. IEEE Energy Conversion Congress and Exposition (ECCE), Montreal, QC, Canada, 20-24 September 2015, pp. 6497-6502.

Daniels B., Gurung J., Huisman H., Lomonova E. A., Feasibility Study of Multi-Phase Machine Winding Reconfiguration for Fully Electric Vehicles, International Conference on Ecological Vehicles and Renewable Energies (EVER), Monte-Carlo, Monaco, 02-10 May 2019, pp: 1-6.

Dubey G. K., Power Semiconductor Controlled Drives. Englewood Cliffs, NJ: Prentice-Hall, 07632, 1989.

Fuchs E. F., Schraud J., Fuchs F. S., Analysis of Critical-Speed Increase of Induction Machines via Winding Reconfiguration with Solid-State Switches. IEEE Transactions on Energy Conversion, 23(3), 774-780, 2008.

Fukuda K., Akatsu K., 5-Phase Double Winding PMSM With Integrated SiC Inverter for in-Wheel Motor, International Conference on Electrical Machines and Systems (ICEMS), Harbin, China, 11-14 August 2019, pp: 1-5.

Gundogdu T., Design and Analysis of Double Fed Interior Permanent Magnet Machines for Traction Applications, IEEE IAS Global Conference on Emerging Technologies (GlobConET), Arad, Romania, 20-22 May 2022, pp: 1036-1042.

Gündoğdu T., Improving the Flux-Weakening Capability of Interior Permanent Magnet Machines by Number of Turns Changing Methodology. Turkish Journal of Science and Technology 17(2), 375-394, 2022.

Hijikata H., Akatsu K., Design Technique and Online Winding Reconfigurations Method of MATRIX Motor, International Power Electronics and Motion Control Conference, Harbin, China, 02-05 June 2012, pp: 713-718.

Im S. H., Park G. M., Gu B. G., Novel Winding Changeover Method for a High Efficiency AC Motor Drive, IEEE Energy Conversion Congress and Exposition (ECCE), Baltimore, MD, USA, 29 Sept. – 03 Oct. 2019, pp: 2347-2352.

Kume T., Iwakane T., Sawa T. Y., Nagai I., A Wide Constant Power Range Vector-Controlled AC Motor Drive Using Winding Changeover Technique. IEEE Transactions on Industry Applications 27(5), 934-939, 1991.

Kume T., Swamy M., A Quick Transition Electronic Winding Changeover Technique for Extended Speed Ranges, IEEE Power Electronics Specialists Conference, Aachen, Germany, 20-25 June 2004, pp: 3384-3389.

Lin M., Li D., Zhao Y., Ren X., Qu R., Improvement of Starting Performance for Line-Start Permanent Magnet Motors by Winding Reconfiguration. IEEE Transactions on Industry Applications 56(3), 2441-2450, 2020.

Maemura A., Morimoto S., Yamada K., Sawa T., Kume T. J., Swamy M. M., A Novel Method for Extending Stroke Length in Moving Magnet Type Linear Motor Drive System by Employing Winding Changeover Technique. IEEJ International Power Electronics Conference, Niigata, Japan, 2005.

Noguchi S., Dohmeki H., Improvement of Torque Ripple Characteristics of Double Winding PMSM with Using Twin Inverters, IEEE International Magnetics Conference (INTERMAG), Singapore, 23-27 April 2018, pp: 1-5.

Sadeghi S., Guo L., Toliyat H. A., Parsa L., Wide Operational Speed Range of Five-Phase Permanent Magnet Machines by Using Different Stator Winding Configurations. IEEE Transactions on Industrial Electronics 59(6), 2621-2631, 2012.

Schraud J., Fuchs E. F., Fuchs H. A., Experimental Verification of Critical-Speed Increase of Single-Phase Induction Machines via Winding Reconfiguration with Solid-State Switches. IEEE Transactions on Energy Conversion 23(2), 460-465, 2008.

Sin S., Ayub M., Kwon B. I., Operation Method of Non-Salient Permanent Magnet Synchronous Machine for Extended Speed Range. IEEE Access 8, 105922-105935, 2020.

Swamy M. M., Kume T. A., Morimoto S., Extended High-Speed Operation Via Electronic Winding-Change Method for AC Motors. IEEE Transactions on Industry Applications 42(3), 742-752, 2006.

Takatsuka Y., Hara H., Yamada K., Maemura A., Kume T., A Wide Speed Range High Efficiency EV Drive System Using Winding Changeover Technique and SiC Devices, International Power Electronics Conference, Hiroshima, Japan, 18-21 May 2014, pp: 1898-1903.

Tang L., Burress T., Pries J. A Reconfigurable-Winding System for Electric Vehicle Drive Applications, IEEE Transportation Electrification Conference and Expo (ITEC), Chicago, IL, USA, 22-24 June 2017, pp: 656-661.